Research Paper 20194087

A Traffic Flow Simulation Framework for Learning Driver Heterogeneity from Naturalistic Driving Data using Autoencoders

Ekim Yurtsever [1)] Chiyomi Miyajima [1)] Kazuya Takeda [1)]

1) Nagoya University, Graduate School of Information Science
Furo-cho, Chikusa-ku, Nagoya, 464-8603, Japan (E-mail: yurtsever.ekim@g.sp.m.is.nagoya-u.ac.jp)

Received on September 12, 2018

ABSTRACT: This paper proposes a novel data-centric framework for microscopic traffic flow simulation with intra and inter driver heterogeneity. We utilized a naturalistic driving corpus of 46 different drivers to learn and model the behavior divergence of Japanese drivers. First, ego-driver behavior signals are used to extract unique features of each driver with an auto-encoder. Then, using these features, drivers are divided into groups using unsupervised clustering algorithms. For each driver group, a feedforward neural network is trained for predicting the desired speed given the road topology. The trained network is then used in a microscopic traffic flow model for simulations. We used a macroscopic traffic survey conducted in Japan to evaluate the proposed framework. Our findings indicate that the proposed framework can simulate a realistic traffic flow with high driver heterogeneity.

KEY WORDS: **Human engineering,** Driver heterogeneity, autoencoder, car-following model, traffic simulation [C2]

1. Introduction

Traffic is a complex multi-agent human-machine network where the nondeterministic nature of human driving styles poses a challenge for modeling. Over the years, various kinds of methods have been developed for modeling the traffic flow[(1)-(4)]. However many of the early works, which used rule-based or physics-based models, disregarded the human diversity in traffic because of the complexity of the problem[(5)].

More recently, several studies proposed various concepts to model the traffic flow heterogeneity [(5)-(13)]. Majority of these employed rule-based approaches. While some of the models can capture certain characteristics of heterogeneous flow, the naturalness of the simulation completely depends on the rules and features designed by the researcher. Furthermore, driver heterogeneity is often generalized, which often leads to the neglection of regional and demographic differences between drivers and the traffic flows. For instance, it is very difficult for a model developed this way to simulate driver heterogeneity realistically in different countries.

With the advancement of data acquisition techniques, information such as speed and acceleration of individual drivers can be collected more easily in comparison to previous decades. This progress led the development of machine-learning based models for traffic simulations[(14)-(16)] and driving behavior analysis[(17)-(18)]. Learning-based models require datasets to be trained and they perform well for imitating particular drivers' car following behaviors. Datasets used for learning-based models can be separated into two groups. The first one comprises detailed ego-behavior signals[(19)-(21)] such as steering and pedal operations, which are crucial for learning particular behavior patterns. However, since these datasets requires an instrumented data collection vehicle to be driven by human subjects, quite often the amount of drivers are low. Therefore, the diversity of the learned behaviors are limited. The second type of datasets include huge amount of drivers but they lack detailed ego-behavior signals. For example, hundreds of vehicles' trajectories on a patch of road network have been collected with a camera on top of a high building in US highway 101 dataset[(22)]. This kind of datasets are very suitable for validating traffic flow simulations but they are insufficient for extracting individual behavior as they lack human input signals such as steering angle and pedal operation.

Our main contribution in this study is a data-centric framework for microscopic traffic simulation that utilizes both kind of datasets for learning intra and inter driver behavior heterogeneity. First, we utilized detailed ego-behavior signals of 46 drivers and used auto-encoder based clustering to group them in an unsupervised manner. The inter-driver heterogeneity comes from these groups. For each group, we trained an feedforward neural network to predict their desired speeds with respect to road topology. We assume that the behavior of an individual driver can be affected by road conditions such as number of lanes, curvature or existence of junctions. The change of car following behavior with respect to these conditions causes intra-driver behavior heterogeneity. We modified a microscopic car following model proposed in[(4)] to be used with the trained networks. The simulated traffic is then compared to a macroscopic traffic survey data for validation.

2. Model Formulation

Homogeneous car following models can be written in the form;

$$v_\alpha(t+T_s) = f\big(v_\alpha(t), \Delta v_\alpha(t), s_\alpha(t)\big) \qquad (1)$$

where v_α is the speed of the αth vehicle in the traffic at time $t+T_s$, Δv_α is the speed difference between the vehicle α and α-1 and s_α is the net distance between vehicle α and α-1. f is modeled differently amongst models. Intelligent driver model[4] (IDM) is regarded as an up-to-date, depictive microscopic car following model in[23]. Furthermore, IDM models the following characteristics with intuitive, human-centric parameters such as desired velocity. This aspect is crucial for us as we use machine learning methods to extract driver behavior from naturalistic data. As such, we utilized IDM in our framework.

2.1. Intelligent Driver Model

Intelligent Driver Model[4] (IDM) models f with two ordinary differential equations:

$$\dot{x}_\alpha = \frac{dx_\alpha}{dt} = v_\alpha \tag{2}$$

$$\dot{v}_\alpha = \frac{dv_\alpha}{dt} = a\left(1 - \left(\frac{v_\alpha}{v_0}\right)^\delta - \left(\frac{s^*(v_\alpha, \Delta v_\alpha)}{s_\alpha}\right)^2\right) \tag{3}$$

$$s^*(v_\alpha, \Delta v_\alpha) = s_0 + v_\alpha T + \frac{v_\alpha \Delta v_\alpha}{2\sqrt{ab}} \tag{4}$$

- v_0: desired velocity
- s_0: desired minimum spacing
- T : desired time headway
- a: maximum vehicle acceleration
- b : comfortable braking deceleration
- δ : an exponent. usually set to 4.
- s_α: distance between vehicle α and α-1

Velocity of each vehicle in the simulation is calculated with the above equations in IDM. In summary, IDM models the free driving behavior, approaching behavior and following in small distance behavior at the same time. For example when the distance to the preceeding vehicle is large, the final term in equation 3 gets a value close to 0. This makes the first term, the free driving term, dominant. IDM is a pure rule-based model without vehicle heterogeneity.

2.2. Proposed Model

We propose a new car-following model based on IDM by including the effect of road topology, $\boldsymbol{u}$, on driving behavior for intra-driver heterogeneity and driving signature $\boldsymbol{o}$ for inter-driver heterogeneity. The general form is shown below:

$$v_\alpha(t+T_s) = f_\alpha\big(v_\alpha(t), \Delta v_\alpha(t), s_\alpha(t), u(\alpha)\big). \tag{5}$$

f_α is the modified IDM, where;

$$\dot{v}_\alpha = a(\boldsymbol{o}_\alpha)\left(1 - \left(\frac{v_\alpha}{v_0^*(\boldsymbol{u}, \boldsymbol{o}_\alpha)}\right)^\delta - \left(\frac{s^*(v_\alpha, \Delta v_\alpha)}{s_\alpha}\right)^2\right) \tag{6}$$

The term $a(\boldsymbol{o}_\alpha)$ and $v^*_0(\boldsymbol{u}, \boldsymbol{o}_\alpha)$ are the modifications we made to the IDM. $a(\boldsymbol{o}_\alpha)$ is the maximum observed acceleration of $\boldsymbol{o}_\alpha$, the driving signature of driver α, and it is extracted from driving data. v^*_0 is a specific function that takes road topology and driving signature as an input and predicts the desired speed. This function is trained via a neural network.

$$v_0^*(\boldsymbol{u}, \boldsymbol{o}_\alpha) = g(\boldsymbol{w}'[\boldsymbol{u}, \boldsymbol{o}_\alpha] + b), \tag{7}$$

where g is a a hyperbolic tangent sigmoid transfer function. Weights $\boldsymbol{w}$ and bias b are learned with conjugate gradient back-propagation. The network is shown in Figure 2.

$\boldsymbol{o}_\alpha$ is the driving signature of driver α and it is obtained with a two-leveled auto-encoder structure. The detailed explanation of extraction of $\boldsymbol{o}_\alpha$ is given below in Section 2.3 and shown in Figure 1.

2.3. Extraction of Driving Signatures

Our goal is to learn the distinct driving style groups in the dataset which can then be imitated in the traffic simulation for heterogeneity. In order to do so we represent each driver with an unique vector. We introduced the term "driving signature" in[24] for this purpose without the extraction method that is proposed in this paper. With driving signatures, drivers can be clustered into similarity groups. In this study we propose to obtain driving signatures through a two-level autoencoder structure.

Overall structure of the two-level autoencoder network is shown in Figure 1. First, we segmented each driver's ego-behavior signals with respect to a change in road topology. A new segment is created for a driver if any of the following has changed during his/her trip: the number of lanes, incoming/outgoing junctions or the curvature of the road (over a threshold). After segmenting, ego-behavior signals have been vectorized as $\boldsymbol{X}_{i,s}$ for driver i at segment s. We used $\boldsymbol{X}$ as the input of the first autoencoder. The idea behind the segmentation is that we want the network to learn to "code" the multi-channel time-series driving data on a particular road topology into a vector $\boldsymbol{z}$.

An autoencoder consists of an encoder and a decoder. This kind of networks try to reconstruct the input data by reducing it to a "code" first. This code can carry the essence of the driving behavior on a segment.

First level autoecnoder:

- $\boldsymbol{X} \rightarrow \boldsymbol{z}$: Encoder-1. Reduces the multi-channel array of driving signals and extracts features, $\boldsymbol{z}$, from the data. Our objective is to learn the features. This is done on a segment basis.
- $\boldsymbol{z} \rightarrow \widehat{\boldsymbol{X}}$: Decoder-1. Tries to reconstruct the data from the code. Both of these networks are trained together with the loss function shown below.

$$E = \frac{1}{N}\sum_{n=1}^{N}\sum_{k=1}^{K}\big(x_{k,n} - \hat{x}_{k,n}\big)^2 + \lambda * \Omega_{\text{weights}} + \beta * \Omega_{\text{sparsity}}, \tag{8}$$

where λ and β are network hyper-parameters, Ω_{weights} is the L_2 regularization term and Ω_{sparsity} is the sparsity regularization term.

The objective of training is to minimize the loss between reconstructed $\widehat{\boldsymbol{X}}$ and the original $\boldsymbol{X}$. We believe that $\boldsymbol{z}$, the

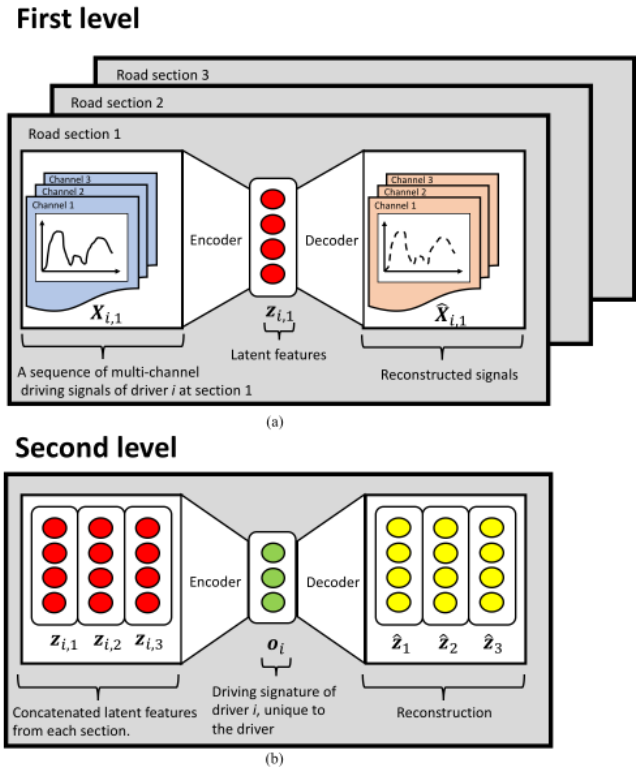

Fig. 1. Learning $\boldsymbol{o}$, the unique driving signature of a driver. (a) First, multi-channel driving data is segmented for each road section. Then, driving signals have been vectorized and fed into the first autoencoder. (b) The latent features learned at each section have been concatenated and used as the input of the second autoencoder. The final latent features are the driving signature $\boldsymbol{o}$ and it is unique to the driver. At this figure, we included only 3 sections for the ease of presentation.

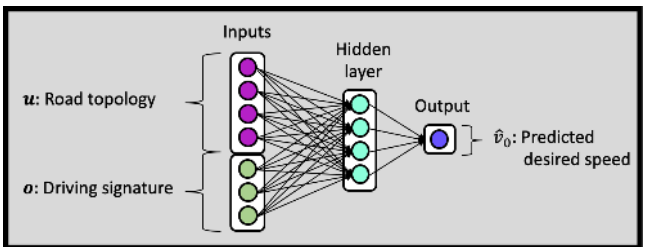

Fig. 2. The fully connected network for predicting the desired speed. Desired speed is predicted with the concatenation of the unique driving signature and road topology.

encoded ego-behavior signals obtained this way, can represent the general behavior of a particular driver at a particular segment.

For the second-level, all codes from all segments that belong to a particular driver, $\boldsymbol{z}_{i,s}|_{s=1,\,2,\,\ldots,\,S}$ are concatenated into a matrix $\boldsymbol{Z}_i$. This new matrix is then fed into a second autoencoder.

Second level autoencoder:

- $Z \rightarrow \boldsymbol{o}$: Encoder-2. Extracts features from the concatenated features of the first level. All level-1 features of a driver are used to create a single vector. This vector is the driving signature, $\boldsymbol{o}$, and it is unique to the driver.

Algorithm 1 Generating the traffic flow

inputs : Probability mass function of driving style groups $p_C(c)$, road topology $U = \{u_1, ..., u_S\}$ and incoming vehicle flowrate function h
outputs: Trajectories of generated vehicles

for *each time step* **do**
  if *it is time to create a new vehicle wtr* f **then**
    generate a vehicle with a counter and driving style group id chosen randomly from p;
    if *the begining of the route is empty* **then**
      place the vehicle on the beginning of the road with an initial speed;
    else
    end
  else
    do not generate a vehicle;
  end
  for *each vehicle generated so far* **do**
    get the road topology that this vehicle is on, u_s;
    update its desired speed with $v_0^*(u_s, C(\text{this vehicle}))$; /* equation 7 */
    if *the road top. is changed from the previous time step for this veh.* **then**
      re-sample the desired speed with a normal distribution with New $v_0^* = \text{normrandom}(\mu, \sigma)$, where $\mu = v_0^*$ and $\sigma = 1$;
    else
      do nothing;
    end
    if *there is a vehicle in front* **then**
      calculate the speed of this vehicle with the modified IDM ; /* equation 6 */
    else if *there is red traffic light in front* **then**
      Assume there is a vehicle with 0 speed at the location of the red light and follow it with the modified IDM;
    else
      assume there is a vehicle 30m in front traveling with the speed limit of the road and follow it with the modified IDM;
    end
  end
end
return trajectory of every vehicle

- $\boldsymbol{o} \rightarrow \hat{Z}$: Decoder-2. Tries to reconstruct $\boldsymbol{Z}$ using $\boldsymbol{o}$. Encoder and decoder are trained together to minimize the loss given in equation 8.

2.4. Predicting desired speed

We assume the desired speed of a driver changes with respect to road topology. This assumption is aligned with studies such as[25] that investigated the effect of road shape on driving behavior. In order to predict the desired speed, $v_0|_{i,s}$, of driver i at road segment s we used a feedforward fully connected network shown in equation 7.

For each road segment, $\boldsymbol{o}_i$, the driving signature of driver i (constant through all segments) and the segments` road topology, $\boldsymbol{u}_s$, have been concatenated as the input of the network. The output of the network is $\hat{v}_0|_{i,s}$. For the supervised training of this network, desired speed $v_0|_{i,s}$, of every driver at each road segment is required. We explained

Fig. 3. The Google Earth image of the experimental route in Nagoya, Japan.

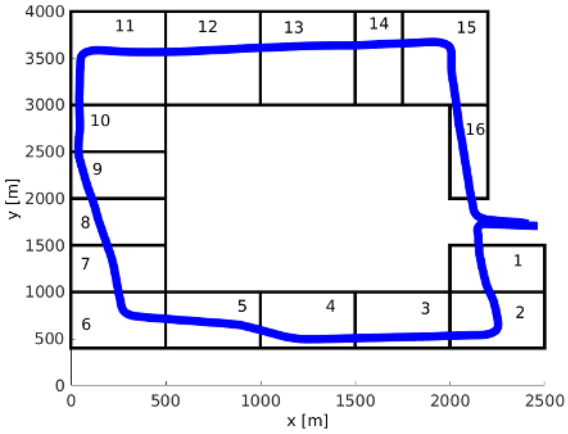

Fig. 4. We divided the route into sections with respect to road topology. A new segment is created if any of the following has changed: the number of lanes, junctions or the curvature of the road.

Table 1 Driving signals

Index	Physical Attributes	Unit
x_1	speed	km/h
x_2	longitudinal acceleration	G
x_3	lateral acceleration	G
x_4	steering wheel angular position	degree
x_5	Force on brake pedal	Newton
x_6	Force on gas pedal	Newton

Table 2 Network structures

Network	Hidden layer size	Transfer function	Hyper-parameters	Training algorithm
Autoencoder-1	25	log sig	$\lambda = 0.001$ $\beta = 1$	scaled conjugate gradient descent
Autoencoder-2:	5	log sig	$\lambda = 0.001$ $\beta = 1$	scaled conjugate gradient descent
FF Network:	10	in: Tansig out: Pure-lin	-	Conjugate gradient back-propagation with Powell-Beale restart

the extraction of desired speed in Section 3 and the network is shown in Figure 2.

2.5. Clustering

Driving signature of all drivers, $O = \{\boldsymbol{o}_1, \boldsymbol{o}_2, \ldots, \boldsymbol{o}_i, \ldots, \boldsymbol{o}_N\}$, are used to find K cluster centroids with K-means algorithm.

With driving signatures O and sets $C = \{c_1, c_2, \ldots, c_j, \ldots, c_K\}$:

$$\text{argmin}_C = \sum_{j=1}^{K} \sum_{\boldsymbol{o} \in c_j} \left\| \boldsymbol{o} - \boldsymbol{\mu}_j \right\|^2. \quad (9)$$

The cluster that driver i belongs to is $C(i) = c_j$ and $\boldsymbol{\mu}_j$ is the cluster centroid. These centroids share a common space with the driving signature $\boldsymbol{o}$.

With clustering, distinct behavior groups that exist in the data are learned. This enables us to generalize the behavior of all drivers that belong to a particular group with the feedforward network.

2.6. Generating Traffic Flow

The modified IDM introduced in equation 6 is used to generate the traffic flow with the trained desired speed predictor. First, the probability mass function of driving style groups p, topology of the road $\boldsymbol{u}$, the incoming vehicle flow rate function h and time step duration are set by the user. Then, the traffic flow is generated with algorithm 1. We used a constant function for h in our implementation. The first generated vehicle needs a lead vehicle in front to follow. This is realized by assuming a vehicle in front traveling with the speed limit of the road. The distance is a parameter of our model and after some trials we found that 30m is an acceptable assumption for urban driving. The distance affects the acceleration behavior of the vehicle.

Using a Gaussian distribution to sample drivers is proposed in[13]. On line 15 of the above algorithm, we resampled the desired speed after predicting it if the driver enters a new road segment. We used the predicted speed as the mean of a normal distribution and resampled it with $\sigma = 1$. This increases the heterogeneity further.

3. Data and Training

3.1. Naturalistic driving corpus

We collected 46 drivers' driving data on Nagoya city in Japan in a one-year period. Each driver followed the same path during the experiment at least twice and each driving session lasted approximately ten minutes. 122 total driving sessions have been held. All the data has been collected with the same vehicle, a Toyota Estima shown in Figure 6.

Seven driving signals obtained from this experiment have been used in this study. These signals are: GPS, speed, longitudinal and lateral acceleration, steering wheel position, force on the brake pedal and the gas pedal. Units of these signals are shown in Table 1. Sampling rate of the GPS is 1 Hz while the original sampling rates of the other signals were 16 kHz. However, in our study those signals are down

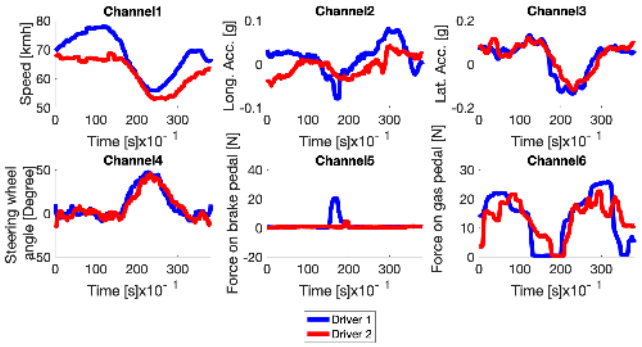

Fig. 5. Sequences of signals collected from 2 different drivers at a curved road segment (segment 2 in Fig. 4). The turning pattern is easy to detect; steering angle and lateral acceleration increases while the speed is decreased for both drivers. Segmenting the signals wtr to road enables us to compare these patterns. Blue driver is a bit more aggressive, he increased his speed (channel 1) just before the curve and had to make a sharp brake (channel 5). Red driver had constant speed before the curve, therefore he made a light brake. Furthermore, blue driver tends to press the brake pedal harder. Our framework clustered these two drivers into different behavior groups. Normalized data have been used in the analysis. However, raw signals (after bias removal) are shown here for the sake of intuitive depiction.

Table 3 Details of the traffic survey

Link ID	Direction	Length [m]	Vehicle flowrate [veh./s]
1	$7 \rightarrow 35$	180	0.3837
2	$34 \rightarrow 8$	450	0.3317
3	$44 \rightarrow 10$	360	0.3836
4	$71 \rightarrow 6$	660	0.2705

sampled at 10 Hz. Examples of the signals are shown in Figure 5. More detailed information about the corpus can be found in[21].

3.2. Defining desired speed

The objective of the feed forward neural network is to estimate the desired speed of each driver group with respect to road topology. Supervised learning is required for this task. Therefore, the desired speed of the training data must be extracted to train the network. Desired speed is the speed the driver wishes to reach given perfect road and free driving conditions. We define the desired speed $v_0|_{i,s}$ for driver i at section s as the following;

$$v_0|_{i,s} = \mu\left(\boldsymbol{X}_{i,s}^{\text{Speed}}\right) + 3\sigma\left(\boldsymbol{X}_{i,s}^{\text{Speed}}\right) \qquad (10)$$

where $\boldsymbol{X}_{i,s}^{\text{Speed}}$ is the sequence of speed signals that is collected from driver i at section s. μ and σ are obtained through fitting a normal distribution to $\boldsymbol{X}_{i,s}^{\text{Speed}}$. In Figure 7, we show an example of a histogram of $\boldsymbol{X}_{i,s}^{\text{Speed}}$ and the fitted distribution. Three-σ rule is widely used in statistics for

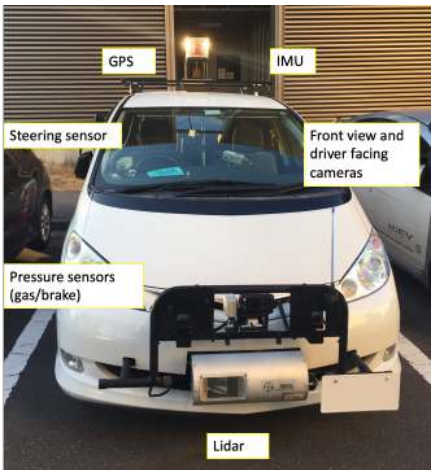

Fig. 6. The instrumented vehicle used for collecting the naturalistic driving data of 46 drivers. The driving group is comprised of 18 females and 28 males and the drivers are aged from 22 to 56 with an average age of 40.5.

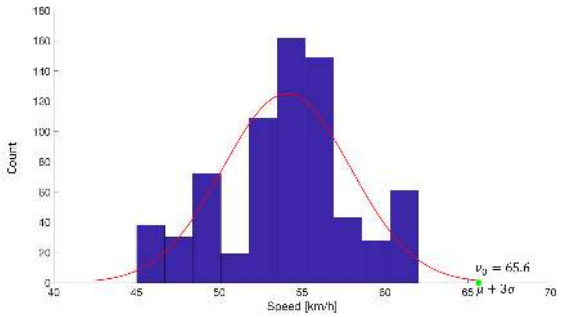

Fig. 7. Histogram of the recorded speed signals of driver m9507A at section 11 and the fitted distribution. Desired speed, v_0(m9507A,11), is 65.6 km/h.

significancy. A result is considered as "significant" if the confidence level is of the order of a three-σ effect. In our case, we believe $\mu + 3\sigma$ can represent the desire of the driver: a speed that is always being aspired but unlikely to be reached

3.3. Network parameters

We employed three neural network structures in our work; autoencoder-1, autoencoder-2 and a fully connected feedforward network. They are mentioned in Section 2 and the structure details are shown in Table 2.

We vectorized the sequence of normalized driving signals for driver i at section s, $\boldsymbol{X}_{i,s}$, into a 1-dimensional vector. For each channel we took 500 samples. If $\boldsymbol{X}_{i,s}$ had less frames than 500, we zero padded the missing frames and trimmed if it had more than 500. After that, we reshaped the 500x6 matrix into a vector of size 3000x1. This one-dimensional vector is the input of autoencoder-1. A vector of 25x1 is obtained (z) as the latent features from the autoencoder. This process is repeated for all sections. In our case we had 15 road segments for testing and 1 for validation, therefore we obtained 15 of these 25x1 vectors. All of these are concatenated and reshaped into a one-dimensional vector of 375x1 for one driver, which is the input of autoencoder-2.

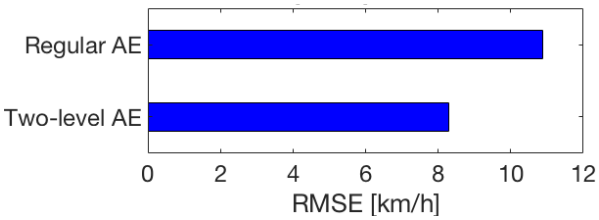

Fig. 8. RMSEs of the predicted desired speeds. Two-level autoencoder outperformed the regular autoencoder.

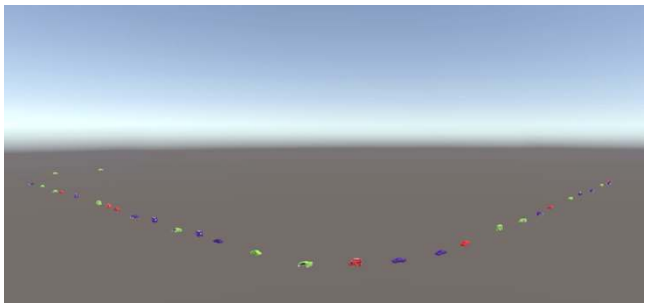

Fig. 9. 3D representation of the simulation. UNITY is used for the visualization. Colors indicate the distinct driving style groups. The complete video is uploaded to: https://youtu.be/ziAyBTLpYnU

A vector with the size of 5x1 is obtained as the latent features from autoencoder-2, which is the driving signature $\boldsymbol{o}_i$ of driver i.

The feedforward network is used to predict the desired speeds. The input of this network is the concatenation of road topology u and driving signature $\boldsymbol{o}_i$. $\boldsymbol{u}$ is a 4x1 vector and $\boldsymbol{o}$ is 5x1. The output is 1x1 $\hat{v}_0$. The network structures are shown in Figure 1, 2 and Table 2.

3.4. Traffic survey data

The benchmark dataset presented in[26] by Horiguchi et al. is utilized to validate the simulated traffic flow. This survey is conducted with more than 200 observers in Tokyo-Kichijoji area. Observers were placed at intersections near the beginning and end the of links and they recorded passing vehicles' license plate numbers with time stamps. Each vehicle's entry and exit time has been logged this way. The resolution of time stamps is 1 minute.

We selected 4 links from this dataset and used it to evaluate the proposed simulation framework. Details of the selected links are shown in Table 3. Direction indicates the nodes and the traffic flow orientation of the link in the Kichijoji benchmark. For example, 7 → 35 stands for the link that starts from the 7th node and ends with the 35th node.

4. Results

The proposed simulation framework has been evaluated in two steps. First, we evaluated the performance of behavior prediction. We compared the predicted desired speeds to the desired speeds obtained from the naturalistic data. For the second step, the macroscopic traffic flow validation, vehicle trajectories of the simulated traffic is compared to the traffic survey data.

Table 4 Car following model parameters

Parameters	Proposed model	IDM with gaussian heterogenity	IDM
v_0 [km/h]	predicted	sampled with gaussian dist. $\mu = 70$	70
s_0 [m]	2	2	2
T [s]	1.5	1.5	1.5
α [m/s^2]	learned from data	sampled with Gaussian dist. $\mu = 1$	1
b [m/s^2]	1.67	1.67	1.67
δ	4	4	4

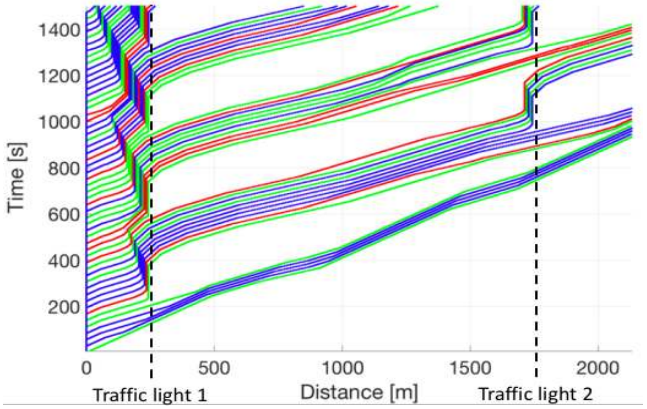

Fig. 10. Traveled distance versus time of each simulated vehicle. Colors indicate the distinct driving style groups. Macroscopic effects of heterogeneity can be seen in this image. There are two traffic lights on this route; one at the 250th meter and the other one in the 1750th meter. When the lights turn red, the first vehicle before the light slows down and comes to a full stop.

4.1. Validation of the behavior prediction

In the first experiment, we examined the performance of the proposed two-level structure against a conventional autoencoder. The driving signals are not segmented with respect to road topology in the conventional structure. All driving signals that belong to driver i, $\boldsymbol{X}_i = (\boldsymbol{X}_{i,1}, \boldsymbol{X}_{i,2}, \dots, \boldsymbol{X}_{i,S})$ is used as the input of a single autoencoder and the latent features obtained from the encoder are used as the driving signatures for the final feedforward network.

Leave-one-out-cross-validation is carried for all road segments. Fifteen segments are used to train the networks and the final segment is used for validation. The held-out ground truth, the desired speed calculated with equation 9, of every driver has been averaged for each cluster. Then, the cluster centroid of each driving style group obtained through training and the held-out segment`s road topology have been concatenated and fed into the trained feedforward network. RMSE of predicted desired speeds of each driving style group with the proposed structure and the conventional autoencoder have been compared in Figure 8. The proposed network outperformed the conventional structure.

We believe the better prediction performance is due to the existence of the inherent differences between drivers and the

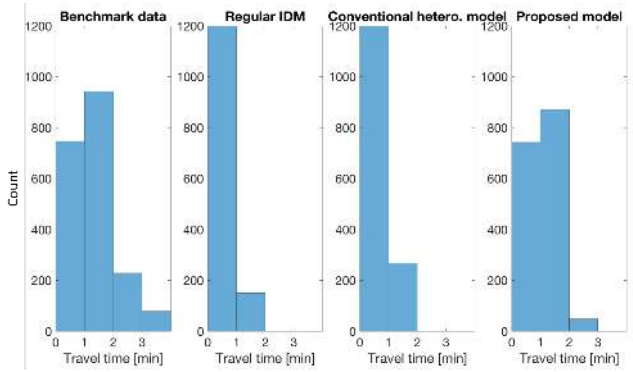

Fig. 11. An example of vehicle travel time histograms (link 2). The proposed framework is the most similar amongst the three methods in comparison to the benchmark data.

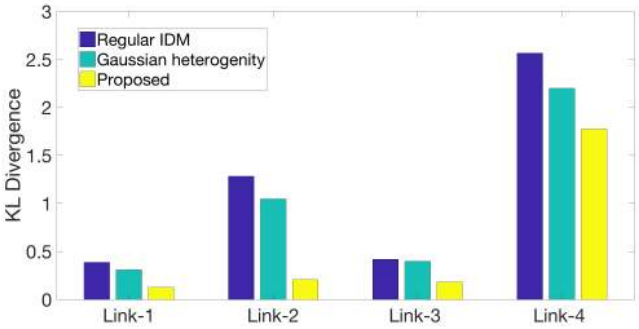

Fig. 12. KL divergence scores of each method in comparison with respect to benchmark data. X axis indicates the link ID. The proposed method generated the most similar traffic flow to the benchmark data on all links

way they change with respect to road topology. The conventional method disregarded these changes. This result shows that the proposed framework is useful for learning the inherent differences between drivers and is able to represent them.

4.2. Validation of the traffic flow

After training the desired speed predictors, we used the traffic generation procedure explained in Algorithm 1. We created a road with different segments, used 3 different driving style groups and ran the simulation. The generated vehicle trajectories are shown in Figure 9 and Figure 10. We used MATLAB for the implementation of the algorithm and UNITY for visualizing the traffic flow. The parameters of the IDM that is used in the proposed network have been showed in Table 4.

In Figures 9 and 10 the colors represent the driving style groups. Figure 9 is a 3D representation of the simulation and Figure 10 shows the traveled distance vs time of each simulated vehicle. In these figures inter driver heterogeneity, the distinctively different characteristics of each group, can be discerned by looking at the following distances. For example, in Figure 9 the green vehicles keep a conservative following distance. In contrast, the red and blue vehicles tend to follow the preceding vehicles very closely. The difference between red and blue vehicles can be seen better in Figure 10; the following behavior of red and blue is affected by the road shape differently. E.g., the red vehicles tend to slow down between the 900th-1300th meters of the route. Intra driver heterogeneity can be noticed especially on the curved road segments. Moreover, realistic macroscopic effects of heterogeneity can be seen as the wave propagation in Figure 10.

In the second traffic flow experiment we measured the simulation accuracy of the proposed method. The conventional IDM without heterogeneity is used as a baseline for comparison. We also compared the proposed algorithm to a conventional heterogeneity model which samples the desired speed of each vehicle with a Gaussian distribution. The parameters used for these methods are also shown in Table 4.

The Tokyo-Kichijoji benchmark traffic survey has been accepted as the ground truth for the simulation accuracy experiment. The initial values of the simulations such as the road topology and incoming traffic flow rate are set as the same with the benchmark data. The remaining initial value, the probability mass function of 3 driving style groups, is set to [0.33 0.33 0.33]. We compared the histogram of travel times of the simulated vehicles with the histogram of the recorded travel time of the surveyed vehicles in the benchmark data.

In Figure 11. an example of four travel time histograms are shown: benchmark data of link 2, simulation with the proposed method, with IDM and with the conventional heterogeneity model. We used KL-divergence score to compare the histograms. The KL-divergence is defined as;

$$D_{\mathrm{KL}}(P \parallel Q) = -\sum_i P(i) \log \frac{Q(i)}{P(i)}, \qquad (11)$$

where P and Q are discrete probability distributions of travel times and i is the histogram bin index. P is the histogram of the survey data and Q is the compared simulation. We normalized the histograms before the comparisons. The KL divergence of the three models in comparison with respect to the benchmark data is shown in Figure 12.

The proposed framework got the lowest KL divergence score with respect to the benchmark data amongst the compared methods. We believe these results show that our framework is capable of generating a realistic traffic flow with heterogeneity learned from naturalistic driving data.

5. Conclusion and future works

A novel framework for utilizing naturalistic driving data to learn heterogeneous driving behavior is proposed in this work. The experiments show that the framework is capable of representing the traffic dynamics of Japan. We believe this framework can be used to learn the driving behavior of different regional and demographic environments if adequate amounts of data is provided. Furthermore, with the rapid development of data acquisition techniques and machine-learning research, data driven methods can become much more effective in the future for traffic simulations.

In this paper we have not used inter-vehicular distances. We intend to use a naturalistic driving dataset with LIDAR and point cloud data in the near future. We believe the use of a large naturalistic driving dataset which consists of ego-signals and surrounding vehicle information together can

increase the data-driven methods performance to a great extent. Our final goal is to develop a pure deep-learning car following model and simulation framework that can be trained for various regional and demographical backgrounds with a data-driven approach.

Acknowledgement

The authors wish to thank Prof. Tetsunori Haraguchi, Prof. Hirofumi Aoki, Prof. Hiroyuki Takashima and Prof. Hiroyuki Okuda of Nagoya University for their fruitful discussions on the topic. This work was partially supported by a Grant-in-Aid for Scientific Research (C) under No.15K002231, from the Japan, Society for the Promotion of Science (JSPS).

References

(1) Newell, G. F. Nonlinear effects in the dynamics of car following. Operations research, Vol. 9, No. 2, pp. 209-229 (1961)
(2) Gipps, P. G. A behavioural car-following model for computer simulation. Transportation Research Part B: Methodological, Vol. 15, No. 2, pp. 105-111 (1981)
(3) Wiedemann, R. Simulation des Strassenverkehrsflusses. (1974)
(4) Treiber, M., Hennecke, A., & Helbing, D. Congested traffic states in empirical observations and microscopic simulations. Physical review E, Vol. 62, No. 2, pp. 1805-1824 (2000)
(5) Ossen, S., & Hoogendoorn, S. P. Heterogeneity in car-following behavior: Theory and empirics. Transportation research part C: emerging technologies, Vol. 19, No.2, pp. 182-195 (2011)
(6) Taylor, J., Zhou, X., Rouphail, N. M., & Porter, R. J. Method for investigating intradriver heterogeneity using vehicle trajectory data: A Dynamic Time Warping approach. Transportation Research Part B: Methodological, Vol. 73, pp. 59-80 (2015)
(7) Lu, X., Wang, Z., Xu, M., Chen, W., & Deng, Z. A personality model for animating heterogeneous traffic behaviors. Computer animation and virtual worlds, Vol. 25, No 3-4, pp. 361-371 (2014)
(8) Chiabaut, N., Leclercq, L., & Buisson, C. From heterogeneous drivers to macroscopic patterns in congestion. Transportation Research Part B: Methodological, Vol. 44, No. 2, pp. 299-308 (2010)
(9) Tang, T. Q., Huang, H. J., Zhao, S. G., & Shang, H. Y. A new dynamic model for heterogeneous traffic flow. Physics Letters A, Vol. 373, No. 29, pp 2461-2466 (2009)
(10) Gundaliya, P. J., Mathew, T. V., & Dhingra, S. L. Heterogeneous traffic flow modelling for an arterial using grid based approach. Journal of Advanced Transportation, Vol. 42, No. 4, pp. 467-491 (2008)
(11) Arasan, V. T., & Koshy, R. Z. Methodology for modeling highly heterogeneous traffic flow. Journal of Transportation Engineering, Vol. 131, No. 7, pp. 544-551 (2005)
(12) Kerner, B. S., & Klenov, S. L. Spatial–temporal patterns in heterogeneous traffic flow with a variety of driver behavioural characteristics and vehicle parameters. Journal of Physics A: Mathematical and General, Vol. 37, No. 37, pp. 8753-8788 (2004)
(13) Wong, G. C. K., & Wong, S. C. A multi-class traffic flow model–an extension of LWR model with heterogeneous drivers. Transportation Research Part A: Policy and Practice, Vol. 36, No. 9, pp. 827-841. (2002)
(14) Kuefler, A., Morton, J., Wheeler, T., & Kochenderfer, M. Imitating driver behavior with generative adversarial networks. In Intelligent Vehicles Symposium (IV), 2017 IEEE, pp. 204-211. (2017)
(15) Lv, Y., Duan, Y., Kang, W., Li, Z., & Wang, F. Y. Traffic flow prediction with big data: a deep learning approach. IEEE Transactions on Intelligent Transportation Systems, Vol. 16, No. 2, pp. 865-873 (2015)
(16) Wang, X., Jiang, R., Li, L., Lin, Y., Zheng, X., & Wang, F. Y. Capturing Car-Following Behaviors by Deep Learning. IEEE Transactions on Intelligent Transportation Systems, Vol. 19, No. 3, pp. 910-920 (2017)
(17) Yamazaki, S., Miyajima, C., Yurtsever, E., Takeda, K., Mori, M., Hitomi, K., & Egawa, M. Integrating driving behavior and traffic context through signal symbolization. In Intelligent Vehicles Symposium (IV), 2016 IEEE, pp. 642-647 (2016)
(18) Yurtsever, E., Yamazaki, S., Miyajima, C., Takeda, K., Mori, M., Hitomi, K., & Egawa, M. Integrating Driving Behavior and Traffic Context Through Signal Symbolization for Data Reduction and Risky Lane Change Detection. IEEE Transactions on Intelligent Vehicles, Vol. 3, No. 3, pp. 242-253 (2018)
(19) Klauer, S. G., Guo, F., Sudweeks, J., & Dingus, T. A. An analysis of driver inattention using a case-crossover approach on 100-car data (No. HS-811 334). (2010)
(20) Benmimoun, M., Pütz, A., Zlocki, A., & Eckstein, L. eurofot: Field operational test and impact assessment of advanced driver assistance systems: Final results. In Proceedings of the FISITA 2012 World Automotive Congress, pp. 537-547, Springer, Berlin, Heidelberg. (2013)
(21) Takeda, K., Hansen, J. H., Boyraz, P., Malta, L., Miyajima, C., & Abut, H. International large-scale vehicle corpora for research on driver behavior on the road. IEEE Transactions on Intelligent Transportation Systems, Vol. 12, No. 4, pp. 1609-1623. (2011)
(22) Colyar, J., & Halkias, J. US highway 101 dataset. Federal Highway Administration (FHWA), Tech. Rep. FHWA-HRT-07-030. (2007)
(23) Sewall, J., Wilkie, D., & Lin, M. C. Interactive hybrid simulation of large-scale traffic. In ACM Transactions on Graphics (TOG), Vol. 30, No. 6, p. 135. ACM. (2011)
(24) Yurtsever, E., Miyajima, C., Selpi, S., & Takeda, K. Driving signature extraction. In Proceedings of the 3rd International Symposium on Future Active Safety Technology Towards Zero Traffic Accidents (FAST-zero 2015), pp.213-217 (2015)
(25) Yurtsever, E., Takeda, K., & Miyajima, C. Traffic trajectory history and drive path generation using GPS data cloud. In Intelligent Vehicles Symposium (IV), 2015 IEEE, pp. 229-234 (2015)
(26) Horiguchi, R., Yoshii, T., Akahane, H., Kuwahara, M., Katakura, M., Ozaki, H., & Oguchi, T. A Benchmark DataSet for Validity Evaluation of Road Network Simulation Models. In Proceedings of 5th World Congress on Intelligent Transport Systems. pp 1-8 (1998)